

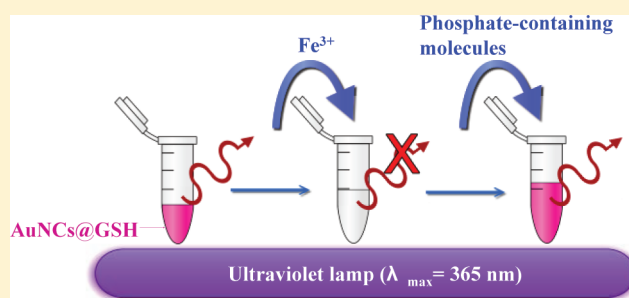
# Using Gold Nanoclusters As Selective Luminescent Probes for Phosphate-Containing Metabolites

Po-Han Li, Ju-Yu Lin, Cheng-Tai Chen, Wei-Ru Ciou, Po-Han Chan, Liyang Luo, Hung-Yu Hsu, Eric Wei-Guang Diau, and Yu-Chie Chen\*

Department of Applied Chemistry, National Chiao Tung University, Hsinchu 300, Taiwan

## S Supporting Information

**ABSTRACT:** Glutathione-bound gold nanoclusters (AuNCs@GSH) can emit reddish photoluminescence under illumination of ultraviolet light. The luminescence of the AuNCs@GSH is quenched when chelating with iron ions (AuNCs@GSH-Fe<sup>3+</sup>), presumably resulting from the effective electron transfer between the nanoclusters and iron ions. Nevertheless, we found that the luminescence of the gold nanoclusters can be restored in the presence of phosphate-containing molecules, which suggested the possibility of using AuNCs@GSH-Fe<sup>3+</sup> complexes as the selective luminescent switches for phosphate-containing metabolites. Phosphate-containing metabolites such as adenosine-5'-triphosphate (ATP) and pyrophosphate play an important role in biological systems. In this study, we demonstrated that the luminescence of the AuNCs@GSH-Fe<sup>3+</sup> is switched-on when mixing with ATP and pyrophosphate, which can readily be observed by the naked eye. It results from the high formation constants between phosphates and iron ions. When employing fluorescence spectroscopy as the detection tool, quantitative analysis for phosphate-containing metabolites such as ATP and pyrophosphate can be conducted. The linear range for ATP and pyrophosphate is 50  $\mu$ M to sub-millimolar, while the limit of detection for ATP and pyrophosphate are  $\sim$ 43 and  $\sim$ 28  $\mu$ M, respectively. Additionally, we demonstrated that the luminescence of the AuNCs@GSH-Fe<sup>3+</sup> can also be turned on in the presence of phosphate-containing metabolites from cell lysates and blood plasma.



Metabolites play an important role in biological systems. For example, adenosine-5'-triphosphate (ATP) is the main energy carrier in cells<sup>1</sup> and also acts as an extracellular signaling agent in many biological processes.<sup>2,3</sup> Pyrophosphate is generated when ATP is hydrolyzed into adenosine monophosphate (AMP). The intracellular concentration of pyrophosphate is  $\sim$ 50  $\mu$ M, while the extracellular concentration of pyrophosphate is  $\sim$ 3  $\mu$ M.<sup>4</sup> In general, the concentration of ATP in cells is at the millimolar level, which is much higher than those of other phosphate-containing metabolites, such as pyrophosphate, adenosine diphosphate (ADP), and AMP.<sup>4,5</sup> It has been known that the level of phosphate-containing metabolites in cells can be used as an indicator of dysfunctions or disorders in biological systems.<sup>6,7</sup> The level of ATP has been used in determination of cell viability.<sup>8</sup> Additionally, the physiologic concentration of blood phosphates in healthy individuals is also at the millimolar level,<sup>9</sup> which is mainly dominated by ATP.<sup>4</sup> Because hypophosphatemia and hyperphosphatemia may result in illness, the phosphate level in blood can be used as an indication for health conditions of individuals.<sup>9</sup> Thus, the development of analytical methods is essential in indicating the level of phosphate-containing metabolites in biological samples.

Traditional ATP assays such as the luciferase assay have been widely used in the determination of ATP levels in vitro.<sup>10–12</sup>

Although the method is sensitive, expensive enzymes and substrates are required for the assays. Thus, efforts have been devoted in designing suitable probe molecules as the sensing probes for ATP<sup>13–15</sup> and pyrophosphate.<sup>16–18</sup> For example, an organic probe composed of a pincer-like benzene-bridge with a pyrene excimer as a signal source and imidazolium as a phosphate anion receptor has been successfully demonstrated as an efficient ATP sensor,<sup>14</sup> while coumarin derivatives have been designed as highly selective fluorescent sensors for pyrophosphate.<sup>18</sup> Electrochemistry<sup>19–21</sup> and spectroscopy<sup>22–33</sup> are commonly employed as analytical tools for the detection of ATP and pyrophosphate. In addition to organic probes, nanoparticles have been used as probes to facilitate the detection process.<sup>26–28</sup> Sensing interactions involve aptamer-based molecular recognition<sup>22–26</sup> and metal ion-based chelation.<sup>29–33</sup>

Glutathione (GSH) is a tripeptide consisting of *N*- $\gamma$ -glutamyl-cysteinyl-glycine and is used as a reducing agent<sup>34–41</sup> for the generation of gold nanoclusters, which has a maximum luminescence at  $\sim$ 613 nm under an excitation of the light at 396 nm (Figure S1 in the Supporting Information).

Received: February 2, 2012

Accepted: May 31, 2012

Published: June 11, 2012

The synthesis of the AuNCs@GSH is quite straightforward by simply stirring aqueous tetrachloroauric(III) acid with GSH for a period of time. The nanoclusters with red luminescence can be readily generated. The generated AuNCs@GSH have good water solubility, stability, and luminescence. In the current study, the use of AuNCs@GSH-Fe<sup>3+</sup> complexes as selective luminescent switches for phosphate-containing metabolites was investigated.

## EXPERIMENTAL SECTION

**Reagents and Materials.** Adenosine monophosphate (AMP), adenosine diphosphate (ADP), adenosine triphosphate (ATP), adenosine, sodium pyrophosphate tetrabasic decahydrate (pyrophosphate), iron(III) chloride hexahydrate (FeCl<sub>3</sub>·6H<sub>2</sub>O), sodium phosphate dibasic (NaH<sub>2</sub>PO<sub>4</sub>), potassium chloride, potassium phosphate monobasic (KH<sub>2</sub>PO<sub>4</sub>), O-phospho-L-tyrosine (phosphor-tyrosine), L-glutathione reduced (GSH), serine, human blood plasma (containing 3.8% trisodium citrate as anticoagulant), and threonine were purchased from Sigma-Aldrich (St. Louis, MO). Ammonium bicarbonate was obtained from J. T. Baker (Phillipsburg, NJ), sodium chloride from Merck (Seelze, Germany), hydrogen tetrachloroaurate(III) hydrate (HAuCl<sub>4</sub>) from Showa (Tokyo, Japan), and trifluoroacetic acid (TFA) from Riedel-de Haën (Seelze, Germany). Millexn GS (pore size, 0.22 μm) and Amicon Ultra-4 (cutoff mass, 3000 Da) filters were purchased from Millipore Filter (Ireland). The adenocarcinoma epithelial A549 cell line (A549) was kindly provided by Prof. RI Chao (National Chiao Tung University), and RAW264.7 macrophages were purchased from the Institute of Food Science (Hsinchu, Taiwan).

**Generation of AuNCs@GSH.** The generation of AuNCs@GSH was mainly based on a protocol described previously.<sup>40,41</sup> In brief, AuNCs@GSH were generated by stirring HAuCl<sub>4</sub> (2.5 mM, 1 mL) and GSH (2.5 mM, 1 mL) at 32 °C under room light for 36 h. Subsequently, 1 mL of GSH (2.5 mM) was added into the reaction, and the mixture was stirred for another 6 h. The resulting solution was centrifuged at 13 000 rpm (rotor radius, 8.3 cm) for 30 min at 4 °C to remove large particles. The supernatant was then filtered using Amicon Ultra-4 filters under centrifugation at 4 500 rpm for 4 h to remove the nonreacted species. The nanocluster solution (~0.5 mL) remaining on the filter was resuspended in deionized water (3 mL) and then centrifuged at 4 500 rpm for 4 h. The rinse steps were repeated three times. The generated nanoclusters have properties similar to those reported in a previous study.<sup>41</sup>

**Preparation of Cell Lysates.** The cultured cells A549 cells and RAW264.7 macrophages (~10<sup>6</sup> cells/mL) were dissolved in a 5 mL of phosphate-buffered saline (PBS) solution containing NaCl (0.137 M), KCl (268 mM), NaH<sub>2</sub>PO<sub>4</sub> (10 mM), and KH<sub>2</sub>PO<sub>4</sub> (1.76 mM). The cells were then centrifuged at 1 000 rpm for 5 min, and the supernatant was removed. The rinse steps were then repeated. The cells were resuspended in a solution (1 mL) of 0.075% TFA/aqueous ammonium bicarbonate (50 mM) (9:1, v/v) and then ultrasonicated for 1 min. The resultant cell lysate was passed through a filter with a pore size of 220 nm. After removing the cell debris, the filtered solution was placed in a centrifuge tube with a filter (cutoff mass, 1000 Da) for centrifugation at 6 000 rpm until no solution remained on the filter. The filtered cell lysate solution was directly used as the sample in the study.

**Instrumentation.** Fluorescence spectra were obtained from a Horiba Jobin Yvon Fluomax-3 spectrofluorometer (Edison, NJ). TEM images were obtained from a JEOL JEM-2100 (Tokyo, Japan) transmission electron microscope (Tokyo, Japan).

## RESULTS AND DISCUSSION

The luminescence of AuNCs@GSH was found quenched in the presence of Fe<sup>3+</sup> (Figure 1) when AuNCs@GSH (10 μL,

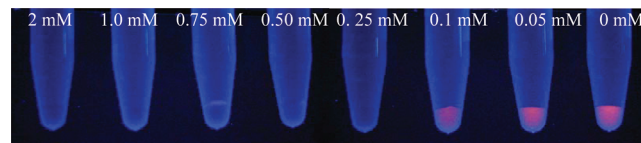


**Figure 1.** Photograph of the AuNCs@GSH (10 μL, 0.756 mM) (under illumination of UV light, λ<sub>max</sub> = 365 nm) following incubation with different concentrations of FeCl<sub>3</sub> solution (10 μL). The concentrations indicated on the figure refers to the initial concentrations of Fe<sup>3+</sup> prior to mixing.

0.756 mM) was vortex-mixed with different concentrations of aqueous FeCl<sub>3</sub> (10 μL) solution for 15 min. The luminescence of AuNCs@GSH gradually decreased and was eventually switched off when the concentration of Fe<sup>3+</sup> reached ~0.25 mM. The quenching effect may have been primarily caused by the binding of Fe<sup>3+</sup> on the surface of AuNCs@GSH because GSH can function as a ligand that chelates with Fe<sup>3+</sup>. Using TEM, the AuNCs@GSH aggregated in the presence of Fe<sup>3+</sup>, whereas no such aggregation was observed when no Fe<sup>3+</sup> was added (Figure 2a). The presence of Fe<sup>3+</sup> caused the aggregation

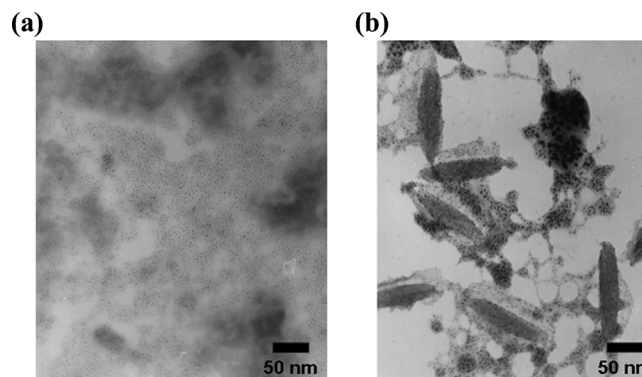


**Figure 2.** TEM images of (a) AuNCs@GSH and (b) AuNCs@GSH-Fe<sup>3+</sup>.

of AuNCs@GSH through the binding of Fe<sup>3+</sup> and AuNCs@GSH (Figure 2b). That is, AuNCs@GSH formed chelate-complexes with Fe<sup>3+</sup>, thereby quenching the luminescence.

The quenching effect presumably results from the effective electron transfer that occurs from AuNCs@GSH complexation with Fe<sup>3+</sup>. The radiative process was not competitive in this case because electron transfer is a very efficient process (<10 ns). The Stern–Volmer plots (Figure 3a) were obtained from steady-state measurements, at which the fluorescence intensity ratios ( $F_0/F$ ) varied as a function of the concentration of FeCl<sub>3</sub> in the AuNCs@GSH solution. The fluorescence intensity of the solution was significantly quenched when the concentration of Fe<sup>3+</sup> in the solution was higher than 0.1 mM. The fluorescence decay of the AuNCs@GSH-Fe<sup>3+</sup> system shows almost identical

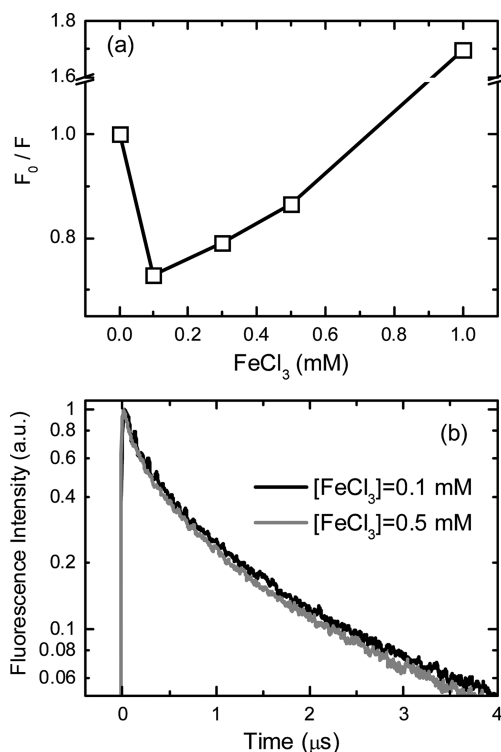
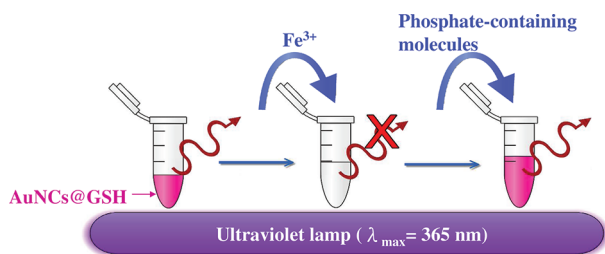


**Figure 3.** (a) Stern–Volmer plots of AuNCs@GSH with adding various concentrations of  $\text{FeCl}_3$  ( $\square$ ). (b) Luminescence decay profiles of AuNCs@GSH excited at 420 nm and probed at 625 nm with the addition of 0.1 and 0.5 mM  $\text{FeCl}_3$ .

decay characteristics (average decay coefficient of  $\sim 2 \mu\text{s}$ , Figure 3b) at the concentrations of 0.1–0.5 mM.

Phosphate anions have high formation constants with  $\text{Fe}^{3+}$ .<sup>42</sup> The formation constant of  $\text{Fe}^{3+}$  with multiphosphates is higher than that with monophosphates because multiple ligands are available for the complexation. Thus, phosphate-containing molecules such as ATP and pyrophosphate were expected to function as good complexation agents for  $\text{Fe}^{3+}$ . Moreover, the luminescence of AuNCs@GSH can be restored in the AuNCs@GSH- $\text{Fe}^{3+}$  solution containing phosphate-containing molecules. On the basis of this characteristic, the AuNCs@GSH- $\text{Fe}^{3+}$  complexes were used as luminescent switches for the detection of phosphate-containing molecules, whose concentrations in a sample can be estimated based on the intensity of the restored luminescence. Scheme 1 displays the graphic representation of the aforementioned sensing method. The switched-off AuNCs@GSH- $\text{Fe}^{3+}$  solution was prepared by adding aqueous  $\text{FeCl}_3$  (0.25 mM, 10  $\mu\text{L}$ ) to an AuNCs@GSH

#### Scheme 1. Cartoon Representation of the AuNCs@GSH- $\text{Fe}^{3+}$ -Based Luminescent Switch for Phosphate-Containing Molecules



solution (0.756 mM, 10  $\mu\text{L}$ ) under vortex-mixing for 15 min. A sample solution was then added to the switched-off solution. The luminescence of the sensing solution can be switched on if the sample contains phosphate-containing molecules. Figure 4

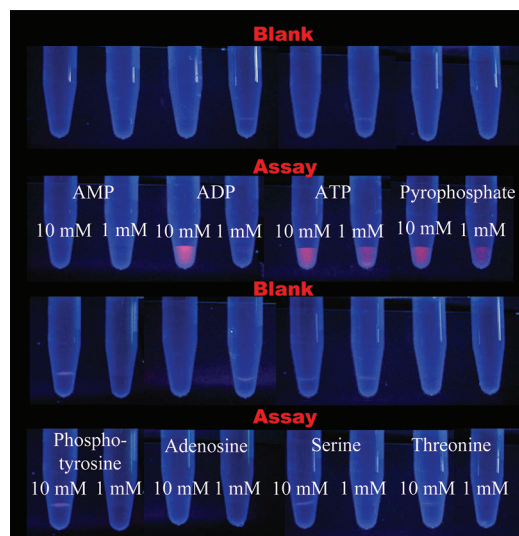


**Figure 4.** Photographs of the AuNCs@GSH- $\text{Fe(III)}$  under UV light ( $\lambda_{\text{max}} = 365 \text{ nm}$ ) (blank, the first and third rows) followed by incubation with different concentrations (10 and 1 mM) of phosphate/nonphosphate-containing molecules. Each “blank” vial contained equal volumes (10  $\mu\text{L}$ ) of AuNCs@GSH (0.756 mM in terms of the concentration of Au) and aqueous  $\text{FeCl}_3$  (0.25 mM). Assay vials (second and fourth rows) were prepared by adding the sample solution (10  $\mu\text{L}$ ) to their corresponding “blank” solution. The label on each tube at the second and fourth rows indicates the initial concentration of the analytes.

displays the photograph of the AuNCs@GSH- $\text{Fe}^{3+}$  solution: the first and third rows were taken under illumination of an ultraviolet lamp ( $\lambda_{\text{max}} = 365 \text{ nm}$ ). The second and fourth rows in Figure 4 were taken after the addition of the samples (1 and 10 mM) into the vials containing AuNCs@GSH- $\text{Fe}^{3+}$ . The luminescence of the AuNCs can be readily switched on with either the addition of 1 mM ATP and pyrophosphate or the addition of 10 mM ADP. The results indicate that multiphosphate-containing molecules such as ATP and pyrophosphate can readily remove  $\text{Fe}^{3+}$  from the surface of AuNCs@GSH, thereby restoring the luminescence of the AuNCs@GSH because  $\text{Fe}^{3+}$  has a high chelating ability with ATP and pyrophosphate.<sup>42,43</sup> ADP can also remove  $\text{Fe}^{3+}$  from the surface of AuNCs@GSH, but a higher concentration is required. Monophosphates such as AMP and phospho-tyrosine at the concentration of 10 mM cannot restore the luminescence of AuNCs@GSH because AuNCs@GSH requires a concentration higher than 10 mM to regain its luminescence. In addition, nonphosphate molecules such as adenosine, serine, and threonine cannot be used to restore the luminescence of the AuNCs@GSH. That is, only molecules containing phosphates can be used to switch on the luminescence of the AuNCs. Furthermore, the results imply that the AuNCs@GSH- $\text{Fe}^{3+}$  is sensitive to phosphate-containing molecules such as ATP and pyrophosphate in a sample.

To explore the feasibility of using this approach for quantitative analysis, fluorescence spectroscopy was used to investigate the response of the sensors toward the concentrations of phosphate-containing metabolites such as ATP and



pyrophosphate. The results show that the concentration–response curve is linear from 50 to 500  $\mu\text{M}$  for ATP ( $y = 302.25x - 13\,076$ ,  $R^2 = 0.9908$ ) (Figure S2 in the Supporting Information) and from 50 to 100  $\mu\text{M}$  for pyrophosphate ( $y = 914.93x - 25\,836$ ,  $R^2 = 0.9862$ ) (Figure S3 in the Supporting Information). However, the limit of detections (LOD) for ATP and pyrophosphate are  $\sim 43\ \mu\text{M}$  and  $\sim 28\ \mu\text{M}$ , respectively, which were calculated according to the assumption of LOD equal to  $3\text{SD}/S$ , where SD is the standard error of the intercept and  $S$  is the slope of the calibration curve.<sup>44,45</sup> Experimental data were treated using Origin 8.0. On the basis of LOD and the slope of the calibration curves, this sensing method is slightly more sensitive toward pyrophosphate than for ATP. However, this method cannot be used to distinguish pyrophosphate from ATP. We also used aqueous disodium hydrogen phosphate ( $\text{Na}_2\text{HPO}_4$ ) as the sample to examine the sensitivity of the  $\text{AuNCs@GSH-Fe}^{3+}$  sensors toward monophosphate anions and observed by fluorescence spectroscopy. There was no fluorescence observed in the fluorescence spectrum when the concentration of the phosphate anions in the sample was lower than 10 mM. Additionally, it is worth noting that pH in the sensing experiment should be adjusted to a weak acidic condition (pH  $\sim 6.5$ ) to prevent precipitation resulting from electrostatic interactions between nanosensors.

As mentioned earlier, the concentration of ATP in cells and human blood plasma is at the millimolar level, which is much higher than those of other phosphate-containing metabolites including pyrophosphate. Although the  $\text{AuNCs@GSH-Fe}^{3+}$  sensors cannot be used to distinguish ATP from pyrophosphate, the sensors can be used to estimate the level of major phosphate containing molecules, i.e., ATP, in complex samples such as cell lysates and blood plasma. Cell lysates were therefore used as the samples based on the current findings, and the performance of  $\text{AuNCs@GSH-Fe}^{3+}$  in sensing the presence of major phosphate-containing metabolites in cell lysate samples was determined. The cell lysates of adenocarcinoma epithelial A549 cell line and RAW264.7 macrophages were used as the model samples. Figure 5 displays the assays obtained before and after the addition of the cell lysate ( $10\ \mu\text{L}$ ,  $10^6$  cells/mL) to the  $\text{AuNCs@GSH-Fe}^{3+}$  solution. The vial shown on the left-hand side of Figure 5 contains the  $\text{AuNCs@GSH}$  solution, which exhibited a bright luminescence under

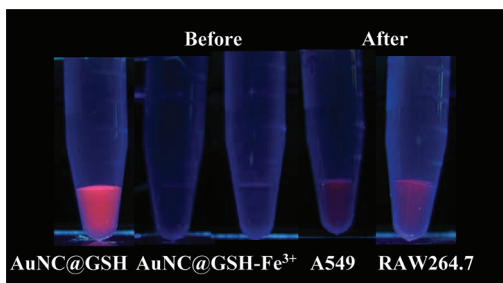


**Figure 5.** Luminescence switched-on assays of the cell lysate samples. The vial on the left-hand side is the  $\text{AuNCs@GSH}$  solution (0.5 mM). The two vials containing  $\text{AuNCs@GSH-Fe}^{3+}$  are labeled “Before.” After adding the cell lysate samples to these two vials and incubating for 30 min, the resultant vials were labeled “After.” The cell lysate samples ( $10\ \mu\text{L}$ ,  $10^6$  cells/mL) included human lung adenocarcinoma epithelial A549 cell line (A549) and RAW264.7 macrophages. The switch-off solution ( $\text{AuNCs@GSH-Fe}^{3+}$ ) was prepared by mixing the  $\text{AuNCs@GSH}$  (0.5 mM,  $40\ \mu\text{L}$ ) and aqueous  $\text{FeCl}_3$  (2.5 mM,  $10\ \mu\text{L}$ ) for 15 min.

illumination of UV light ( $\lambda_{\text{max}} = 365\ \text{nm}$ ). After the addition of  $\text{Fe}^{3+}$  to the solution, the luminescence was switched off (labeled as “Before” in Figure 5). The cell lysates of A549 and RAW 264.7 were then individually added to two vials containing  $\text{AuNCs@GSH-Fe}^{3+}$ . The light was “turned on” in the vials labeled as “After”, although the light was not as bright as the original  $\text{AuNCs@GSH}$ . The results demonstrate that the current approach can be used to detect the presence of major phosphate-containing molecules in cell lysates. Since ATP is the major phosphate containing metabolites in the cells and has been used as a biomarker for determination of cell viability,<sup>8</sup> the current approach can be potentially used as an alternative method for this purpose.

Additionally, we also used the  $\text{AuNCs@GSH-Fe}^{3+}$  as the sensing probes to estimate the ATP level in a human plasma sample. Although our sensors are especially sensitive to ATP and pyrophosphate, the concentration of pyrophosphate is much lower than that of ATP in blood.<sup>4</sup> Thus, we assumed that ATP in the blood plasma would be responsible for the turn-on effect in the  $\text{AuNCs@GSH-Fe}^{3+}$ -based sensing approach. We used the standard addition method by spiking different amounts of ATP to a 70-fold diluted human plasma to estimate the ATP level in the sample. The sensors were slightly turned on when mixing with the diluted plasma sample (the spectrum marked in a green color in Figure S4 in the Supporting Information). As the concentration of additional ATP increases, the emission intensity at the maximum wavelength of  $\sim 613\ \text{nm}$  increases. On the basis of the standard addition results, we estimated the concentration of ATP in the plasma is  $\sim 3\ \text{mM}$  (Figure S4 in the Supporting Information). Although we do not have the information of the concentration of ATP in the plasma, the estimated value is in the range that is known in human blood plasma.<sup>9</sup>

## CONCLUSIONS

In conclusion, a facile sensing method for phosphate-containing metabolites using  $\text{AuNCs@GSH-Fe}^{3+}$  as the sensing probes was demonstrated. The results indicate that this sensing approach is especially sensitive to ATP and pyrophosphate. These phosphate-containing molecules are the most abundant metabolites in cells; thus, the proposed sensing approach can be used to rapidly examine the levels of phosphate-containing metabolites in cell lysates, which can be potentially used as an indication of cell viability and cell metabolic activity. Additionally, it is also possible to use this sensing probe in the estimation of the level of phosphate in biological fluids such as blood plasma. ATP is one of the major components in blood plasma; therefore, the change in the ATP level in the blood plasma may be used as an indicator of disorders. Thus, we have demonstrated the possibility by directly using the  $\text{AuNCs@GSH-Fe}^{3+}$  as the sensors to estimate the ATP level in a blood plasma sample. The range was estimated at the millimolar level, which is similar to the range known in human blood plasma. The main advantages of this approach: (1) The probes are easily prepared. (2) The sensing experiment is easily conducted. Unlike the traditional luciferase assay, no expensive chemicals are required. The sensing experiment simply results from a one-step competitive chelating process, which only takes 15 min to achieve equilibrium. Thus, simplicity and speed are the two main features of this sensing method. To populate the method further, efforts can be devoted in the development of a microarray-based platform for high-throughput analysis.

**■ ASSOCIATED CONTENT****■ Supporting Information**

Additional information as noted in text. This material is available free of charge via the Internet at <http://pubs.acs.org>.

**■ AUTHOR INFORMATION****Corresponding Author**

\*E-mail: [yuchie@mail.nctu.edu.tw](mailto:yuchie@mail.nctu.edu.tw). Phone: 886-3-5131527. Fax: 886-3-5723764.

**Notes**

The authors declare no competing financial interest.

**■ ACKNOWLEDGMENTS**

P.-H.L., J.-Y.L., and C.-T.C. contributed equally to this work. We thank the National Science Council (NSC) of Taiwan for financial support of this work. We also thank Prof. Pawel L. Urban for helpful discussions of the data treatment for quantitative analysis.

**■ REFERENCES**

- (1) Knowles, J. R. *Annu. Rev. Biochem.* **1980**, *49*, 877–919.
- (2) Azorin, N.; Raoux, M.; Rodat-Despoix, L.; Merrot, T.; Delmas, T. P.; Crest, M. *Exp. Dermatol.* **2011**, *20*, 401–407.
- (3) Hardie, D. G.; Hawley, S. A. *Bioessays* **2001**, *23*, 1112–1119.
- (4) Sakamoto, T.; Ojida, A.; Hamachi, I. *Chem. Commun.* **2009**, 141–152.
- (5) Griffiths, E. J.; Halestrap, A. P. *Biochem. J.* **1993**, *290*, 489–495.
- (6) Pettegerew, J. W.; Keshavan, M. S.; Panchalingam, K.; Strychor, S.; Kaplan, D. B.; Tretta, M. G.; Allen, M. *Arch. Gen. Psychiatry* **1991**, *48*, 563–568.
- (7) Brandon, M.; Baldi, P.; Wallace, D. C. *Oncogene* **2006**, *25*, 4647–4662.
- (8) Schmidt, J.; Mueller, U.; Wallimann, C.; Mathes, S.; Probst, C.; Siegrist, S.; Andretta, C.; Leist, C.; Graf-Hausner, U. *BioProcess Int.* **2008**, *6*, 46–54.
- (9) Levi, M.; Popovtzer, M. Disorders of phosphate balance. In *Atlas of Diseases of the Kidney*; Berl, T., Bonventre, J. V., Eds.; Current Medicine, Inc.: Philadelphia, PA, 1999; Vol. 1, Chapter 7.
- (10) Kangas, L.; Grönroos, M.; Nieminen, A. L. *Med. Biol.* **1984**, *62*, 338–343.
- (11) Lundin, A.; Hasenson, M.; Persson, J.; Pousette, A. *Methods Enzymol.* **1986**, *133*, 27–42.
- (12) Petty, R. D.; Sutherland, L. A.; Hunter, E. M.; Cree, I. A. J. *Biolumin. Chemilumin.* **1995**, *10*, 29–34.
- (13) Zhou, Y.; Xu, Z.; Yoon, J. *Chem. Soc. Rev.* **2011**, *40*, 2222–2235.
- (14) Xu, Z.; Singh, N. J.; Lim, J.; Pan, J.; Kim, H. N.; Park, S.; Kim, K. S.; Yoon, J. *J. Am. Chem. Soc.* **2009**, *131*, 15528–15533.
- (15) Jeon, H.; Lee, S.; Li, Y.; Park, S.; Yoon, J. *J. Mater. Chem.* **2012**, *22*, 3795–3799.
- (16) Kim, S. K.; Lee, D. H.; Hong, J. I.; Yoon, J. *Acc. Chem. Res.* **2009**, *42*, 23–31.
- (17) Ha Na Lee, H. N.; Xu, Z.; Kim, S. K.; Swamy, K. M. K.; Kim, Y.; Kim, S.-J.; Yoon, J. *J. Am. Chem. Soc.* **2007**, *129*, 3828–3829.
- (18) Kim, M. J.; Swamy, K. M. K.; Lee, K. M.; Jagdale, A. R.; Kim, Y.; Kim, S.-J.; Yoo, K. H.; Yoon, J. *Chem. Commun.* **2009**, 7215–7217.
- (19) Xu, Y. D.; Venton, B. J. *Electroanalysis* **2010**, *22*, 1167–1174.
- (20) Reynes, O.; Bucher, C.; Moutet, J. C.; Royal, G.; Saint-Aman, E. *Inorg. Chim. Acta* **2008**, *361*, 1784–1788.
- (21) Aranzaes, J. R.; Belin, C.; Astruc, D. *Angew. Chem., Int. Ed.* **2006**, *45*, 132–136.
- (22) Kanekiyo, Y.; Naganawa, R.; Tao, H. *Chem. Commun.* **2004**, 1006–1007.
- (23) Yushchenko, O.; Vadzyuk, B.; Kosterin, S. O.; Duportail, G.; Mely, Y.; Pivovarenko, V. G. *Anal. Biochem.* **2007**, *369*, 218–225.
- (24) Su, S.; Nutiu, R.; Filipe, C. D. M.; Li, Y.; Pelton, R. *Langmuir* **2007**, *23*, 1300–1302.
- (25) Wang, J.; Jiang, Y. X.; Zhou, C. S.; Fang, X. H. *Anal. Chem.* **2005**, *77*, 3542–3546.
- (26) Bogomolova, A.; Aldissi, M. *Biosens. Bioelectron.* **2011**, *26*, 4099–4103.
- (27) Chen, Z.; Li, G.; Zhang, L.; Jiang, J. F.; Li, Z.; Peng, Z. H.; Deng, L. *Anal. Bioanal. Chem.* **2008**, *392*, 1185–1188.
- (28) Callan, J. F.; Mulrooney, R. C.; Karnila, S. J. *Fluoresc.* **2008**, *18*, 1157–1161.
- (29) Moro, A. J.; Cywinski, P. J.; Körsten, S.; Mohr, G. J. *Chem. Commun.* **2010**, *46*, 1085–1087.
- (30) Sakamoto, T.; Ojida, A.; Hamachi, I. *Chem. Commun.* **2009**, 141–152.
- (31) Yu, F.; Li, L.; Chen, F. *Anal. Chim. Acta* **2008**, *610*, 257–262.
- (32) Shtykov, S. N.; Smirnova, T. D.; Bylinkin, Y. G. *J. Anal. Chem.* **2004**, *59*, 438–441.
- (33) Foy, G. P.; Pacey, G. E. *Talanta* **1996**, *43*, 225–232.
- (34) Wilcoxon, J. P.; Martin, J. E.; Parsapour, F.; Wiedenman, B.; Kelley, D. F. *J. Chem. Phys.* **1998**, *108*, 9137–9143.
- (35) Schaaff, T. G.; Knight, G.; Shafiqullin, M. N.; Borkman, R. F.; Whetten, R. L. *J. Phys. Chem. B* **1998**, *102*, 10643–10646.
- (36) Alvarez, M. M.; Khoury, J. T.; Schaaff, T. G.; Shafiqullin, M. N.; Vezmar, I.; Whetten, R. L. *J. Phys. Chem. B* **1997**, *101*, 3706–3712.
- (37) Schaaff, T. G.; Shafiqullin, M. N.; Khoury, J. T.; Vezmar, I.; Whetten, R. L.; Cullen, W. G.; First, P. N. *J. Phys. Chem. B* **1997**, *101*, 7885–7891.
- (38) Hostetler, M. J.; Wingate, J. E.; Zhong, C. J.; Harris, J. E.; Vachet, R. W.; Clark, M. R.; Londono, J. D.; Green, S. J.; Stokes, J. J.; Wignall, G. D.; Glish, G. L.; Porter, M. D.; Evans, N. D.; Murray, R. W. *Langmuir* **1998**, *14*, 17–30.
- (39) Schaaff, T. G.; Whetten, R. L. *J. Phys. Chem. B* **2000**, *104*, 2630–2641.
- (40) Zheng, J. Ph.D. Dissertation, Georgia Institute of Technology, Atlanta, GA, 2005.
- (41) Chen, C.-T.; Chen, W.-J.; Liu, C.-Z.; Chang, L.-Y.; Chen, Y.-C. *Chem. Commun.* **2009**, 7515–7517.
- (42) Childs, C. W. *J. Phys. Chem.* **1969**, *73*, 2956–2960.
- (43) Al-Sogair, F.; Marafie, H. M.; Shuaib, N. M.; Youngo, H. B.; El-ezaby, M. S. *J. Coord. Chem.* **2002**, *55*, 1097–1109.
- (44) Miller, J. N.; Miller, J. C. *Statistics and Chemometrics for Analytical Chemistry*; Prentice Hall: Harlow, England, 2000.
- (45) Urban, P. L.; Garca-Ruiz, C.; Garcia, M. A.; Marina, M. L. *J. Sep. Sci.* **2005**, *28*, 2200–2209.